Designing aryl cations for direct observation in solution: *ab initio* MO calculations of UV spectra

David M. Smith,†[a] Zvonimir B. Maksic[a] and Howard Maskill[b]

[a] *Quantum Organic Chemistry Group, Rudjer Boskovic Institute, 10000 Zagreb, Croatia*
[b] *Department of Chemistry, University of Newcastle, Newcastle upon Tyne, UK NE1 7RU*

Received (in Cambridge, UK) 23rd January 2002, Accepted 12th March 2002
First published as an Advance Article on the web 10th April 2002

A detailed study of the vertical UV/visible spectra of the phenyl cation and some derivatives has been undertaken to identify an aryl cation which, when produced by dediazoniation, will be observable by laser flash photolysis. Calculations on the phenyl cation itself confirmed that it has no strongly allowed transition in the desired region of the spectrum. It was found that the primary effect of heteroatom substitution external to the ring upon the spectrum arose from the alteration of existing orbital energies. Particularly important was the effect of the heterosubstituent on the energy of the empty σ orbital, located on the dehydro carbon. Also important was the polarisation of π orbitals by the substituent and, in some cases, the configurational mixing of states of lower symmetry. Several externally substituted systems showed promise in terms of being potentially observable; however, in the cases where the transitions were in the right region of the spectrum, the intensities were rather modest and, when transitions were calculated to possess large intensities, they were not usually in the most convenient UV spectral range. Internal heteroatom substitution leading to heterocyclic aryl cations was also investigated. As well as the alteration of orbital energies, polarisation of the π space, and configurational mixing, this type of substitution perturbed the spectrum of the phenyl cation in an additional way: new transitions involving the excitation of non-bonding electrons appeared. In the majority of cases, however, the heterocyclic cations did not exhibit particularly strong transitions in the desired spectral region; an exception was the pyrimidin-5-yl cation which was calculated to possess a particularly promising electronic state (1-^1A_1) but its diazonium ion precursor is synthetically inaccessible. Externally substituted pyrimidin-5-yl cations were calculated to show a persistently strong n–σ transition in the 270–290 nm wavelength range. In the 2-amino-4-hydroxypyrimidin-5-yl cation, the intensity of this transition was particularly high, and the precursor arenediazonium ion appears to be synthetically accessible.

Introduction

There have been many attempts to identify and characterise aryl cations with some success in mass spectrometric gas phase experiments[1] and in solid matrices at very low temperatures.[2] From such work, some thermodynamic, structural, and spectroscopic properties have been measured, and some information has been obtained regarding gas phase reactivity.[1] Aryl cations (Ar^+) have also been invoked,[3] and denied,[4] as intermediates in dediazoniation reactions in solution at normal temperatures, but have eluded detection by laser flash photolysis (LFP) methods so far.[5,6] The problems are two-fold. First, there is good evidence that singlet aryl cations are generated by flash photolysis of arenediazonium ions, but that they are extremely short-lived.[6] Secondly, the usual detection method in LFP is UV spectroscopy, and simple singlet aryl cations have only very weakly absorbing chromophores in easily accessible parts of the UV spectrum. Detection of Ar^+ by LFP in solution would allow its reactivity with the solvent and solutes to be investigated, *i.e.* its bimolecular reactivity rather than static properties. This has already been achieved with vinyl cations.[7]

Regardless of experimental difficulties in proving the existence of aryl cations in solution, theoretical studies have continued. Taft first proposed a high degree of radical-cation character in the transition state for dediazoniation reactions due to transfer of a π electron from the benzene ring into the vacant σ (sp^2) orbital of the incipient carbocation.[8] The triplet electronic state was claimed to be more stable than the corresponding singlet, but early semi-empirical and *ab initio* molecular orbital calculations were not supportive although results depended upon substituents.[9] Subsequent high level *ab initio* studies confirmed a singlet ground state phenyl cation and a less stable, very short-lived triplet.[10–12]

We now report results of an investigation of the absorption spectra of various derivatives of the phenyl cation using current *ab initio* molecular orbital theory. The aim of this endeavour was to identify aryl cations possessing easily observable electronic transitions (measurable absorbances at wavelengths longer than *ca.* 250 nm in dilute solution). The results will allow better informed attempts at the generation of aryl cations from corresponding arenediazonium ions under LFP conditions. If successful, this combination of theory and experiment will allow characterisation of solvated aryl cations, and structure–reactivity investigations in solution.

Theoretical procedures

The phenyl cation (**1**) and selected derivatives (**2**–**16**) are shown in Fig. 1. In order to calculate the UV/vis spectrum for each of these molecules, the geometry of the lowest singlet state was first optimised using the CASSCF/6-31G(d) procedure with either the GAUSSIAN 94,[13] or MOLPRO 2000[14] program suites. Rather than choosing a single active space to apply to all molecules, each molecule was considered individually. For example, the active space for the parent phenyl cation (**1**) consisted of six electrons in seven orbitals (abbreviated in the following by 6,7). The seven orbitals correspond to three bonding π orbitals (containing the six electrons), three antibonding π

† *Present address*: Department of Chemistry, Ludwig Maximilians University, Butenandt-Str. 5-13, D-81377 Munich, Germany.

 DOI: 10.1039/b200898j

This journal is © The Royal Society of Chemistry 2002

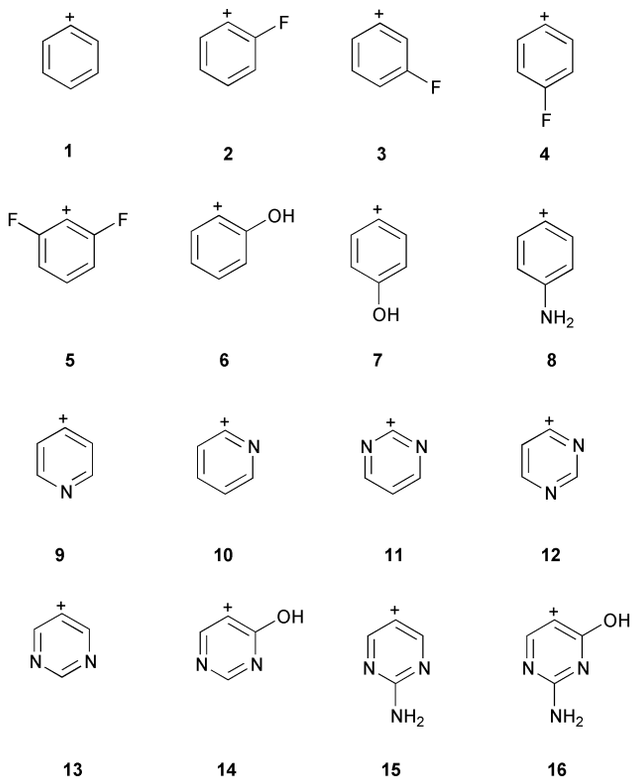

Fig. 1 The phenyl cation and selected derivatives investigated in this work.

orbitals, and one empty σ (sp^2) orbital at the site of the missing hydrogen. Each of the derivatives shown in Fig. 1 was treated with at least this minimal active space. However, in most cases it was deemed necessary to add supplementary electrons and/or orbitals to obtain a satisfactory description. The chosen active spaces are included with the tables of results and will be discussed individually below.

Using the optimised geometry of the lowest singlet state obtained according to the above procedure, further single point calculations were carried out to determine the features of the vertical UV/vis spectrum. The CASPT2/cc-pVDZ theoretical method as available in MOLCAS 5.0[15] was chosen to carry out these calculations. The active spaces for the CASSCF reference functions for this part of the investigation were generally the same as that chosen for geometry optimisation. In some cases, however, problems with intruder states were encountered in the perturbation expansion and the relevant active space had to be enlarged to compensate. Specific information on these cases can again be found in the tables of results and as part of the general discussion below.

In many cases, only the lowest state of a given symmetry was considered to be important. In this event, the CASSCF orbitals were optimised for the state of interest and the multi-reference second-order perturbation treatment applied, under the single-state formalism, without issue. When the calculation of more than one state of a given symmetry was required, the CASSCF orbitals were optimised for an evenly weighted average of the states of interest and the "multi-state" option of MOLCAS 5.0 was utilised in the perturbation treatment.[16] This latter feature enables excited states of the same symmetry to interact under the perturbation and thus gives a more realistic estimate of the state energies. In all cases, the lowest singlet (ground) state was calculated as an individual state and the resulting energy used as the reference value for the calculation of excitation energies. The notation used throughout the paper is standard but deserves a brief comment for the sake of clarity. The symbol 2-^3A_2 is used to describe the second excited triplet state of A_2 symmetry (in the C_{2v} point group). The first excited singlet state of A′ symmetry (in the C_s point group) appears as $1\text{-}^1A'$.

Transition intensities were also computed and are presented in terms of the oscillator strength (f). The transition dipole moment values required for the calculation of f were obtained from the "State Interaction" module of MOLCAS 5.0 using the CASSCF wave functions. This procedure allows computation of transition properties between non-orthogonal states and thus permits the wave function of the individually optimised ground state (see above) to be used to calculate transition properties to all other states. In cases where more than one state of a given symmetry was considered, the perturbatively mixed CASSCF wave functions, generated from the multi-state CASPT2 calculations,[16] were used for the calculation of transition properties.

When the ground electronic state is a singlet, transitions to triplet states (and even certain singlet states) are electric-dipole forbidden. In our endeavour to design a potentially visible derivative of the phenyl cation, these states are not of specific interest. Nevertheless, we have presented excitation energies for selected forbidden transitions as it can help in understanding the effect of various substitutions on the spectrum as a whole.

Results and discussion

The phenyl cation

It is now generally agreed that the lowest electronic state of the phenyl cation is a singlet ($^1A_1$) with the lowest triplet ($^3B_1$) state *ca.* 80–100 kJ mol^{-1} higher in energy.[10–12] However, the singlet–triplet gap is a property strongly dependent on geometry. This is evident, for example, in the relatively large differences in adiabatic and vertical ionisation energies of the phenyl radical, particularly to the singlet state.[10,11] Furthermore, even though the singlet state is calculated to lie lower in energy than the triplet state at the phenyl radical geometry, the geometry difference between the two states is such that the Franck–Condon factors actually favour the formation of the triplet in the ionisation process.[11]

Given the strong geometry dependence of the singlet–triplet gap in the phenyl cation, it is clear that some care must be exercised when selecting geometries for the calculation of vertical UV/vis spectra. As we are attempting to design observable cations to be generated in a dediazoniation reaction, it would seem sensible to consider the geometric aspects of this process. Glaser and co-workers[17] have demonstrated that the bonding in the benzenediazonium ion is best described as a dative interaction between an essentially neutral N_2 group and a singlet phenyl cation. Our own investigations, as well of those of Glaser and co-workers,[18] show that as the dediazoniation reaction proceeds (on the singlet electronic surface), the geometry of the hydrocarbon fragment increasingly resembles that of the isolated singlet phenyl cation. It seems that, if the phenyl cation is formed as an intermediate in the decomposition of benzenediazonium salts, it is generated in the optimum geometry of the lowest singlet state. Therefore, this geometry seems the best choice as a reference point from which to calculate vertical UV/vis spectra of the phenyl cation and selected derivatives for potential observation in LFP experiments. Details of the vertical UV/vis spectra of the phenyl cation calculated in this way are shown in Table 1. The first point of interest is the good agreement obtained between the cc-pVDZ and the cc-pVTZ results. The largest discrepancy between the λ_{max} predictions of the two basis sets is only 13.0 nm (3.9 kJ mol^{-1} or 0.04 eV) for the $^1B_1$ state. The calculated oscillator strengths also exhibit a very low basis set dependence. These results, combined with analogous comparisons for several of the other systems in Fig. 1 (results not shown), indicate that the economical cc-pVDZ basis set is adequate for the task at hand.

The spectrum in the region considered can be seen to be dominated by transitions from the occupied π orbitals to the empty σ (sp^2) orbital on the dehydro carbon (designated as π–σ

Table 1 Vertical UV/vis spectrum of the phenyl cation (**1**) calculated using a (6,7) active space

State	Assignment	λ_{max}/nm	*f*
cc-pVDZ			
$^1A_2$	π–σ	670.24	0.00000
$^1B_1$	π–σ	627.24	0.00019
$^1B_2$	π–π*	252.60	0.00003
$^1A_1$	π–σ	186.58	0.00921
$^3B_1$	π–σ	797.33	
$^3A_2$	π–σ	673.50	
cc-pVTZ			
$^1A_2$	π–σ	674.29	0.00000
$^1B_1$	π–σ	640.29	0.00018
$^1B_2$	π–π*	258.24	0.00004
$^1A_1$	π–σ	190.52	0.00966
$^3B_1$	π–σ	802.46	
$^3A_2$	π–σ	679.73	

Table 2 Vertical UV/vis spectrum of the 2-fluorophenyl cation (**2**) calculated using a (6,8) active space

State	Assignment	λ_{max}/nm	*f*
1-$^1A''$	π–σ	1420.50	0.00007
2-$^1A''$	π–σ	919.81	0.00017
3-$^1A''$	π–σ	308.37	0.00138
1-$^1A'$	π–σ	272.98	0.00511
2-$^1A'$	π–σ	253.68	0.00677
3-$^1A'$	π–π*, π–σ	245.47	0.00251
1-$^3A''$	π–σ	1802.29	
2-$^3A''$	π–σ	1093.47	

transitions). The lowest of these, as expected, is the transition to the $^3B_1$ state. The transition to the $^1B_1$ state occurs at a considerably shorter wavelength than that to the $^3B_1$ state, while the $^1A_2$ and $^3A_2$ states are predicted to be almost isoenergetic. These findings are in agreement with previous calculations,[10] albeit at a different geometry. A significant feature of the spectrum for the purposes of the current work, however, is the absence of a strongly allowed transition in the desired region of the spectrum. In the following sections, we address the question of how to design a suitable derivative of the phenyl cation which possesses a more easily observable excitation.

Heterosubstitution external to the ring

We began our search by considering simple heterosubstitution external to the ring, the first example of which is provided by the 2-fluorophenyl cation (**2**). The active space chosen for this compound consisted of six electrons in eight orbitals (*i.e.*, 6,8 as opposed to 6,7 for **1**). The extra orbital was an antibonding σ orbital (σ*) which displayed strong spatial overlap with the empty σ (sp^2) orbital of the dehydro carbon. Due to the frequent interchanging of these two orbitals in the calculations, it was decided to include both in the active space to avoid further problems. The natural orbital occupancy of this additional antibonding σ orbital was always small and its effect on the results negligible. However, its intrusion in the calculations was not confined to the 2-fluorophenyl cation (**2**) but remained a consistent feature of many other molecules. In all cases where this orbital was found to interfere, it was added to the active space. The inclusion of the lone pair orbitals of fluorine in the active space was investigated and found to have little or no effect on either the geometry or the computed spectrum.

The most obvious feature of the spectral details shown in Table 2 is the appreciable red shift of the first few π–σ transitions. This arises because of the substantial stabilisation of the vacant σ orbital by the adjacent fluorine atom (from −0.18 hartree to −0.21 hartree), which reduces the energy required for π–σ excitations. Another important effect of the fluorine is the polarisation of the π orbitals. This polarisation implies that certain transitions involving these orbitals will have larger transition dipole moments than in the unsubstituted phenyl cation. In general, this will translate into larger oscillator strengths. A further effect that can serve to magnify transition intensities is the mixing of the electronic configurations due to the reduction of symmetry. This latter effect is best demonstrated by the composition of the wave function of the 3-$^1A'$ state. The largest contributions to this wave function arise from electronic configurations corresponding to π–π* excitations. However, there are also significant contributions from π–σ configurations. Although the transition to this state appears at virtually the same wavelength as that of the corresponding π–π* transition in **1**, the configurational mixing apparent in **2** allows the π–σ configurations to contribute to the magnification of the transition intensity. The combination of this effect with the polarisation of the π orbitals leads to an oscillator strength for the π–π* transition in **2** that is two orders of magnitude larger than for the analogous transition in **1**. Add to this the stabilisation of the vacant σ orbital and the spectrum as a whole is changed so that two potentially observable transitions appear. That is, the transitions to the 3-$^1A''$ and 1-$^1A'$ states lie within the desired wavelength range and possess non-zero intensities. However, the predicted oscillator strengths are not very high, and perhaps a better alternative is available.

Table 3 Vertical UV/vis spectrum of the 3-fluorophenyl cation (**3**) calculated using a (6,8) active space

State	Assignment	λ_{max}/nm	*f*
1-$^1A''$	π–σ	845.93	0.00000
2-$^1A''$	π–σ	644.28	0.00012
3-$^1A''$	π–σ	263.89	0.00155
1-$^1A'$	π–π*	250.34	0.00243
2-$^1A'$	π–σ	195.08	0.00700
1-$^3A''$	π–σ	898.48	
2-$^3A''$	π–σ	756.24	

Table 4 Vertical UV/vis spectrum of the 4-fluorophenyl cation (**4**) calculated using a (6,8) active space

State	Assignment	λ_{max}/nm	*f*
1-$^1B_1$	π–σ	755.38	0.00026
1-$^1A_2$	π–σ	652.02	0.00000
2-$^1B_1$	π–σ	264.27	0.00128
1-$^1B_2$	π–π*	259.34	0.00100
$^1A_1$	π–σ	206.86	0.00773
2-$^1A_2$	π–σ	193.03	0.00000
2-$^1B_2$	π–σ	181.05	0.01252
$^3B_1$	π–σ	1029.70	
$^3A_2$	π–σ	616.89	

It appears that fluorosubstitution at either the 3- or 4-position offers no improvement in terms of our desired purpose. Tables 3 and 4 show the calculated spectral details for the 3-fluorophenyl (**3**) and 4-fluorophenyl (**4**) cations, respectively. The active spaces for these compounds were chosen to be the same as for **2** above. Examination of the energies for excitation to the lowest π–σ singlet states in each case shows that the fluorine becomes less effective, in terms of stabilising the vacant σ orbital, the further away it is. Nevertheless, in all of the monofluorophenyl cations, the lowest π–σ transition is predicted to occur at a longer wavelength than in the unsubstituted parent (**1**). The 3-$^1A''$ state of **3** and the 1-$^1B_1$ state of **4** are both potentially observable in LFP experiments but it would seem that the 2-fluorophenyl cation (**2**) offers a better prospect than either of these two compounds.

Due to the potential success of the 2-fluorophenyl cation, it was decided to investigate the 2,6-difluorophenyl cation (**5**). Again, a six electron, eight orbital active space was employed.

Table 5 Vertical UV/vis spectrum of the 2,6-difluorophenyl cation (**5**) calculated using a (6,8) active space

State	Assignment	λ_{max}/nm	f
1-$^1A_2$	π–σ	9168.30	0.00000
1-$^1B_1$	π–σ	1912.37	0.00014
2-$^1B_1$	π–σ	388.00	0.00139
1-$^1B_2$	π–σ	345.38	0.00488
1-$^1A_1$	π–σ	338.19	0.00522
2-$^1A_1$	π–σ	267.96	0.00000
2-$^1B_2$	π–π*	259.12	0.00924
2-$^1A_2$	π–σ, π–π*	226.88	0.00000
$^3B_1$	π–σ	9455.82	
$^3A_2$	π–σ	7555.16	

Table 6 Vertical UV/vis spectrum of the 2-hydroxyphenyl cation (**6**) calculated using a (6,8) active space

State	Assignment	λ_{max}/nm	f
1-^{1}A″	π–σ	1857.60	0.00005
2-^{1}A″	π–σ	824.79	0.00018
3-^{1}A″	π–σ, π–π*	333.37	0.00128
1-^{1}A′	π–σ	282.13	0.00494
2-^{1}A′	π–π*	272.78	0.00629
3-^{1}A′	π–σ	245.56	0.00251
1-^{3}A″	π–σ	2650.18	
2-^{3}A″	π–σ	985.70	

Inspection of the lowest energy transitions in Table 5 shows that the inclusion of two fluorine atoms adjacent to the dehydro carbon stabilises the empty σ orbital to an even greater extent than a single fluorine. The effect on the σ orbital energy is roughly additive, as evidenced by its value of −0.24 hartree in **5**. Due to the higher symmetry of the 2,6-difluorophenyl cation, the contribution of configurational mixing is less than in **2**. However, the polarisation of the π orbitals is greater and the end result is that the predicted oscillator strengths in **5** and in **2** are of comparable magnitudes. The 1-$^1B_2$ and 2-$^1A_1$ states of **5** both show promise but, as was the case with **2**, the intensities of the transitions leading to them are still modest and perhaps more suitable alternatives may present themselves.

To determine the effect of the nature of the external substituent on the spectrum of **1**, calculations on selected hydroxyphenyl cations were undertaken. Table 6 shows the calculated spectral details of the 2-hydroxyphenyl cation (**6**). The positions of the lowest energy transitions in **6** (compared to those in **2**) indicate that the hydroxy substituent is more efficient, in terms of stabilising the σ orbital, than is fluoro substitution. However, the spectrum of **6** as a whole is predicted to be very similar to that of **2**. The potentially observable transitions for **6** (those leading to the 3-^{1}A″, 1-^{1}A′, and 2-^{1}A′ states) are slightly red-shifted with respect to those for **2**, and there is more π–π* character in this region of the spectrum. The intensities, however, are much the same. The 2-hydroxyphenyl cation (**6**) may be a slightly better candidate for observation than **2**, but the difference is not great.

Comparison of the low energy transitions in the 4-hydroxyphenyl cation (**7**, Table 7) and in **4** reinforces the above conclusion regarding stabilisation of the vacant σ orbital by the hydroxy group. The 1-^{1}A′ state in **7** (λ_{max} = 292.08 nm, f = 0.01022) represents the most promising candidate yet. The extra intensity associated with the transition to this state, compared with that in **4**, arises because of the lower symmetry of **7** (C_s instead of C_{2v}). As mentioned before, this symmetry lowering allows intensity to be borrowed *via* the process of configurational mixing.

The 4-aminophenyl cation (**8**) required a treatment slightly different to the other externally substituted systems we considered. The active space for this molecule consisted of eight

Table 7 Vertical UV/vis spectrum of the 4-hydroxyphenyl cation (**7**) calculated using a (6,8) active space

State	Assignment	λ_{max}/nm	f
1-^{1}A″	π–σ	1294.97	0.00010
2-^{1}A″	π–σ	753.59	0.00000
1-^{1}A′	π–σ	292.08	0.01022
3-^{1}A″	π–σ	283.86	0.00109
2-^{1}A′	π–π*	253.02	0.00630
1-^{3}A″	π–σ	2013.56	
2-^{3}A″	π–σ	725.82	

Table 8 Vertical UV/vis spectrum of the 4-aminophenyl cation (**8**)[a] calculated using an (8,8) active space

State	Assignment	λ_{max}/nm	f
1-^{1}A′[b]	π–σ	1350.52	0.00983
1-^{1}A″	π–σ	1027.66	0.00203
2-^{1}A′[b]	π–σ	520.62	0.02759
3-^{1}A′[b]	π–π*	366.39	0.02319
2-^{1}A″	π–π*, π–σ	314.15	0.01504
4-^{1}A′[b]	π–σ, π–π*	301.00	0.00244
3-^{1}A″	π–σ	278.29	0.00961
5-^{1}A′[b]	π–π*, π–σ	253.15	0.28280
^{3}A″	π–σ	891.31	

[a] Note that the symmetry plane of this molecule bisects the phenyl ring consequently, the meanings of A′ and A″ are slightly different. Also, as mentioned in the text, the ground state is actually the ^{3}A′ triplet which lies 30.8 kJ mol^{-1} below the lowest singlet (from which the above transitions are calculated). [b] Calculated with a (12,10) active space due to intruder state problems.

electrons in eight orbitals (8,8). This choice encompasses one extra orbital and two additional electrons to include the lone pair of electrons on nitrogen, which was found to have a strong influence on the calculations. The antibonding σ orbital that was found to interfere on previous occasions did not do so in this case, and was therefore omitted from the active space. Optimisation of the geometry of **8** revealed one particularly interesting feature. In agreement with the previous (single reference) calculations of Glaser,[18] the phenyl ring was predicted to be nonplanar with the dehydro carbon puckered out of the plane containing all the other ring atoms. Unlike the single-reference calculations, the CASSCF level predicts a C_s structure, with a plane bisecting the ring and a planar NH_2 group, to be a minimum. In this situation, the meanings of the irreducible representations A′ and A″ are slightly different for **8** from those for the C_s structures discussed previously.

In accordance with the nitrogen's sp^2 hybridisation, its lone pair assumes a substantial p-character. Rather than forming a localised C=N double bond, this p-type lone pair orbital combines with all of the π orbitals and contributes to a π system that extends throughout the entire molecule. The electron pair in the HOMO in this case, however, most closely resembles a lone pair of electrons on the dehydro carbon. All these characteristics combine to make the spectrum of **8** quite different from those of the previously discussed systems. The first and most obvious feature is that the lowest triplet state actually lies lower than the lowest singlet state (Table 8), even at the optimised geometry of the singlet. Although there is some stabilisation of the empty σ orbital by the NH_2 substituent, this energetic reversal primarily arises from the energetic destabilisation of the HOMO, as well as the large spatial overlap between the HOMO and the LUMO. The fact that the triplet state is lower in energy does not necessarily imply that **8** is not a good candidate for observation. That is, the formation of the triplet state in the dediazoniation reaction would require intersystem crossing at some point on the reaction path. This is not always a favourable process and we have, therefore, calculated the vertical spectrum from the geometry of the singlet, as before.

Table 9 Vertical UV/vis spectrum of the pyridin-4-yl cation (**9**) calculated using an (8,8) active space

State	Assignment	λ_{max}/nm	*f*
1-^1A_2	π–σ	623.80	0.00000
1-^1A_1	n–σ	584.87	0.04727
1-^1B_1	π–σ	391.52	0.00022
1-^1B_2	π–π*	236.07	0.01035
2-^1B_1	π–σ	220.75	0.00048
$^3A_1$	n–σ	675.20	
$^3B_1$	π–σ	628.25	
$^3A_2$	π–σ	457.66	

Using the 8,8 active space, some problems were encountered with the perturbative calculations on the states of A′ symmetry. In particular, the $4\text{-}^1A'$ and $5\text{-}^1A'$ states exhibited very low weights of the CASSCF reference wave functions because of certain terms that gave too large a contribution to the second-order energy due to small energy denominators. By enlarging the active space to encompass the orbitals associated with these small energy denominators (two further occupied orbitals of A′ symmetry to give a 12,10 active space), the low reference weights were eliminated and the calculations deemed reliable.

Table 8 shows that, under the chosen computational scheme, the 4-aminophenyl cation (**8**) possesses several strongly allowed transitions. In particular, transitions to the $3\text{-}^1A'$, $2\text{-}^1A''$, and $4\text{-}^1A'$ states show significant promise in terms of being observed. However, the impracticability of generating a simple aminoarenediazonium ion precursor to the 4-aminophenyl cation (**8**) may render this candidate unsuitable.

Internal heterosubstitution

We now turn to the consideration of a different type of heterosubstitution of the phenyl cation, *i.e.*, internal heterosubstitution, leading to various hetero-aromatic cations. Our initial investigations focussed on the pyridin-4-yl cation (**9**), the chosen active space of which consisted of eight electrons in eight orbitals. As with the 4-aminophenyl cation (**8**), this space was composed of one doubly occupied orbital for the lone pair of electrons on nitrogen and the 6,7 space chosen for the parent phenyl cation. As was the case with all hetero-aromatic derivatives, the antibonding σ orbital did not interfere with the calculations and so was omitted from the active space. The inclusion of the lone pair of electrons in the active space was not found to have a large effect on the geometry of the pyridin-4-yl cation (**9**), but the calculated spectrum was quite sensitive to their presence.

The lowest π–σ transitions shown in Table 9 can be seen to be blue shifted with respect to those in the phenyl cation. This is because the presence of the heteroatom in the ring actually destabilises the vacant σ orbital. Table 9 also shows why it is important to include the lone pair of electrons in the active space for the hetero-aromatic derivatives of the phenyl cation: the absorbance leading to the 1-^1A_1 state involves the excitation of a non bonding (n) electron to the empty σ orbital (an n–σ transition). This transition is relatively strongly allowed but, in this case, occurs at rather too long a wavelength for the purpose in mind. Inclusion of the heteroatom adjacent to the charge, as in the pyridin-2-yl cation (**10**), does nothing to improve the situation (Table 10). This repositioning of the heteroatom can be seen to destabilise further the empty σ orbital, as reflected by the wavelengths calculated for the lowest transitions. The quite large destabilisation in this case translates into an absence of any transitions carrying significant intensity in the desired region. Transitions involving nonbonding electrons occur at wavelengths shorter than 220 nm and are not shown in Table 10.

Compounds involving two nitrogens in the ring have the potential to be more suitable than the aforementioned pyridinyl cations. Our first attempt at such a system was the pyrimidin-2-yl cation (**11**). To include both of the lone pairs of this compound into the active space requires a total of ten electrons and nine orbitals, and this was the active space chosen to obtain the optimum geometry of **11**. However, further problems were encountered with intruder states in the perturbative calculations for this ion and it was decided to enlarge the active space to fourteen electrons in eleven orbitals for the purposes of calculating the spectrum. The positions of the lowest π–σ transitions in Table 11 show that the empty σ orbital is again destabilised by the presence of the nitrogens in the ring. However, several transitions involving excitations from the nonbonding electrons appear in the Table. The absorption leading to the 1-^1B_2 state represents one potentially observable n–σ transition. The lowest energy n–π* transition carries reasonable intensity but appears at too short a wavelength. The transition to the π–π* state derives significant intensity from its relatively large n–σ character, but its position is also less than ideal.

The pyrimidin-4-yl cation (**12**) represents a slight improvement. The added distance between the dehydro carbon and one of the nitrogen atoms lessens the destabilisation of the empty σ orbital (Table 12). Consequently, the lowest energy n–σ transition is potentially observable. The n–π* transition in this case is predicted to be relatively weak, while the π–π* transition is associated with a large oscillator strength but appears at rather a short wavelength.

Intruder states were again found to interfere with the calculation of the spectrum for the pyrimidin-5-yl cation (**13**). The 10,9 active space incorporating both lone pairs was found to be

Table 10 Vertical UV/vis spectrum of the 2-pyridinyl cation (**10**) calculated using an (8,8) active space

State	Assignment	λ_{max}/nm	*f*
$1\text{-}^1A''$	π–σ	395.31	0.00049
$2\text{-}^1A''$	π–σ	330.25	0.00001
$^1A'$	π–π*	236.92	0.01120
$^3A''$	π–σ	430.73	
$^3A'$	π–π*	306.81	

Table 11 Vertical[a] UV/vis spectrum of the pyrimidin-2-yl cation (**11**) calculated using a (14,11) active space

State	Assignment	λ_{max}/nm	*f*
1-^1B_2	n–σ	314.38	0.00704
1-^1B_1	π–σ	300.21	0.00047
2-^1B_1	n–π*	256.26	0.00799
1-^1A_2	π–σ	250.68	0.00000
2-^1B_2	π–π*, n–σ	241.89	0.07019
1-^1A_1	n–σ	195.71	0.00257
2-^1A_2	n–π*	193.88	0.00000
$^3B_1$	π–σ	313.35	
$^3B_2$	π–π*	286.82	
$^3A_1$	π–π*	259.02	
$^3A_2$	π–σ	257.31	

[a] Geometry obtained using a (10,9) active space.

Table 12 Vertical UV/vis spectrum of the pyrimidin-4-yl cation (**12**) calculated using a (10,9) active space

State	Assignment	λ_{max}/nm	*f*
$1\text{-}^1A'$	n–σ	370.60	0.06402
$1\text{-}^1A''$	π–σ	364.36	0.00027
$2\text{-}^1A''$	π–σ	264.38	0.00000
$3\text{-}^1A''$	n–π*	257.89	0.00165
$2\text{-}^1A'$	π–π*	224.60	0.01287
$^3A'$	n–σ	442.45	
$^3A''$	π–σ	367.27	

Table 13 Vertical[a] UV/vis spectrum of the pyrimidin-5-yl cation (**13**) calculated using a (14,11) active space

State	Assignment	λ_{max}/nm	f
1-$^1B_2$	n–σ	893.13	0.01039
1-$^1B_1$	π–σ	430.84	0.00091
2-$^1B_1$	n–π*	355.14	0.00602
1-$^1A_2$	π–σ	350.17	0.00000
2-$^1A_2$	n–π*	290.17	0.00000
1-$^1A_1$[b]	n–σ	275.26	0.08384
2-$^1B_2$	π–π*	249.43	0.01870
$^3B_2$	n–σ	1217.37	
$^3B_1$	π–σ	507.99	
$^3A_1$	n–σ	405.65	
$^3A_2$	π–σ	348.28	

[a] Geometry obtained using a (10,9) active space. [b] Calculated with a (16,12) active space due to an intruder state problem.

sufficient for geometry optimisation. As with the pyrimidin-2-yl cation (**11**), a 14,11 active space was chosen for the spectrum and found to alleviate all problems bar one. That is, the 1-$^1A_1$ state required an active space comprising sixteen electrons in twelve orbitals to eliminate all intruder state problems. The positioning of both nitrogens *meta* to the dehydro carbon further lessens the destabilisation of the vacant σ orbital. The transitions to the lowest excited singlet and triplet states are actually found to occur at longer wavelengths than in the phenyl cation (Table 13). However, in this case, these lowest transitions are of n–σ and not π–σ nature. The n–π* transition is predicted to be relatively weak, while the π–π* transition is again at too short a wavelength. However, the second n–σ transition (to 1-$^1A_1$) is very well-positioned (λ_{max} = 275.26 nm) and is associated with quite a large oscillator strength (f = 0.08384). This transition has by far the most potential to be observed of any discussed so far.

As with the 4-aminophenyl cation (**8**), however, the extremely promising pyrimidin-5-yl cation (**13**) seems to be associated with some practical difficulties. That is, 5-aminopyrimidine has been reported not to give a diazonium salt under standard conditions[19,20] and so the reactant in the dediazoniation experiment appears to be inaccessible. However, derivatives of 5-aminopyrimidine are readily diazotized[21] so a combination of internal and external heterosubstitution has the potential to result in a synthetically accessible arenediazonium ion leading to an aryl cation with an observable UV/vis spectrum. Such possibilities are investigated in the following section.

Combined internal and external heterosubstitution

The first externally substituted hetero-aromatic ion to be considered was the 4-hydroxypyrimidin-5-yl cation (**14**). It was found that a minimal 6,7 active space was sufficient for the geometry optimisation of this system. The larger 10,9 active space containing the nitrogen lone pairs was used for the calculation of the spectrum. The presence of the hydroxy group shifts the lowest n–σ transitions to a shorter wavelength (Table 14). The lowest energy π–σ transitions, on the other hand, are predicted to appear at a longer wavelength in **14** than in **13**. These shifts are a consequence of the hydroxy group destabilising the highest non-bonding orbital, while at the same time stabilising the vacant σ orbital. Importantly, the strong n–σ transition remains, albeit with some added π–π* character. The intensity of this transition is reduced compared with the analogous one in **13**, but it is still sizeable and potentially observable.

The 2-aminopyrimidin-5-yl cation (**15**) required twelve electrons in ten orbitals for a consistent treatment. That is, the inclusion of the NH_2 lone pair in the active space was found to be important, as was observed previously for the

Table 14 Vertical[a] UV/vis spectrum of the 4-hydroxypyrimidin-5-yl cation (**14**) calculated using a (10,9) active space

State	Assignment	λ_{max}/nm	f
1-$^1A'$	n–σ	811.76	0.01251
1-$^1A''$	π–σ	505.71	0.00093
2-$^1A''$	π–σ	389.19	0.00062
3-$^1A''$	n–π*	309.22	0.00292
2-$^1A'$	n–σ, π–π*	274.22	0.03448
$^3A'$	n–σ	953.35	
$^3A''$	π–σ	645.86	

[a] Geometry obtained using a (6,7) active space.

Table 15 Vertical UV/vis spectrum of the 2-amino-5-pyrimidinyl cation (**15**) calculated using a (12,10) active space

State	Assignment	λ_{max}/nm	f
1-$^1B_1$	π–σ	1507.32	0.00063
1-$^1B_2$	n–σ	1380.20	0.00383
1-$^1A_2$	π–σ	390.97	0.00000
2-$^1B_2$	π–π*, n–σ	367.08	0.04542
2-$^1B_1$	n–π*	355.40	0.00012
1-$^1A_1$	π–σ	307.17	0.00055
2-$^1A_1$[a]	n–σ, π–π*	287.43	0.08979
$^3B_1$	π–σ	2358.93	
$^3B_2$	n-σ	1546.14	
$^3A_1$	n-σ, π–σ	419.36	
$^3A_2$	π–σ	385.82	

[a] Calculated with a (16,12) active space due to an intruder state problem.

4-aminophenyl cation (**8**). On this occasion, however, the presence of an sp^2 hybridized external nitrogen was not sufficient to distort the ring from planarity, and C_{2v} symmetry was realised. The lowest energy transition to a singlet state is of π–σ nature on this occasion (Table 15), reflecting the destabilising influence of the amino substituent on the highest occupied π orbital. Two transitions arise with mixed n–σ and π–π* character. The first (to 2-$^1B_2$) is primarily a π–π* transition and is predicted to have quite a large oscillator strength. The second (to 2-$^1A_1$) is the persistent n–σ transition from **13** and, as was the case in **14**, it has a little π–π* character mixed in. The wavelength (λ_{max} = 287.43 nm) and intensity (f = 0.08979) associated with this transition seem to be ideal for the task at hand.

The final compound considered in this study combines all of the favourable spectroscopic features previously discussed. That is, the 2-amino-4-hydroxypyrimidin-5-yl cation (**16**) is a combination of the potentially successful 2-hydroxyphenyl, 4-aminophenyl, and pyrimidin-5-yl cations. Table 16 shows how the positive features of these systems combine to produce a very promising compound. A 12,10 active space, containing the three nitrogen lone pairs, was found to be necessary for geometry optimisation. Again, the ring was found to prefer planarity, despite the presence of an amino substituent opposite the charged site. Intruder states were frequently encountered during the excited state calculations and it was decided to compute the entire spectrum using an enlarged (14,11) active space.

The transition to the lowest π–σ singlet state occurs at quite a long wavelength. This is due to the stabilisation of the empty σ orbital (by the hydroxy substituent) working in combination with the destabilisation of the highest occupied π orbital (by the amino substituent). In addition, the hydroxy substituent causes the lowest n–σ transition to be shifted to a shorter wavelength compared with **15**. Table 16 also shows that the region of spectroscopic interest is filled with allowed transitions, several of them associated with quite large oscillator strengths. The

Table 16 Vertical[a] UV/vis spectrum of the 2-amino-4-hydroxypyrimidin-5-yl cation (**16**) calculated using a (14,11) active space

State	Assignment	λ_{max}/nm	f
1-^{1}A″	π–σ	2769.06	0.00043
1-^{1}A′	n–σ	1155.66	0.00011
2-^{1}A″	π–σ	553.76	0.00000
3-^{1}A″	n–σ	380.69	0.00035
2-^{1}A′	π–σ	360.26	0.00125
3-^{1}A′	n–σ, π–π*	324.27	0.04302
4-^{1}A″	n–π*, π–σ	322.72	0.00305
5-^{1}A″	n–π*, π–σ	305.52	0.00231
4-^{1}A′	n–σ, π–π*	281.22	0.17643
^{3}A″	π–σ	6916.26	
1-^{3}A′	n–σ	1324.52	
2-^{3}A′	π–σ	399.74	

[a] Geometry obtained using a (12,10) active space.

configurational mixing due to the lower symmetry of this ion is clearly making a contribution here.

The transitions mixing n–σ and π–π* character are again of most importance. The transition to the 3-^{1}A′ state exhibits quite promising characteristics. However, the transition to the 4-^{1}A′ state is even more attractive. This strongly allowed n–σ transition is consistently found between 270 and 290 nm in all of the pyrimidin-5-yl cation derivatives considered. In the case of the 2-amino-4-hydroxypyrimidin-5-yl cation (**16**) the substituents work together in such a way that the intensity of this transition is maximised (f = 0.17643), and achieves a very high value indeed. In terms of its calculated spectrum, compound **16** thus represents the system with the highest chance of being observed in dediazoniation experiments.

Perhaps the most impressive feature of compound **16**, however, is its potential synthetic accessibility. That is, 2,5-diamino-4-hydroxy-6-methylpyrimidine (**17**, Scheme 1) was found to be

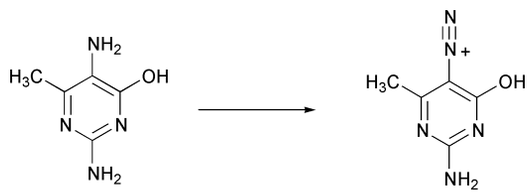

17 **18**

Scheme 1 The diazotization of 2,5-diamino-4-hydroxy-6-methylpyrimidine.

easily diazotized to give a diazonium salt with the diazo group in the 5-position (**18**, Scheme 1).[22] This latter compound was found to undergo normal dediazoniation reactions. We did not perform calculations including the methyl group at the 6-position, but it is anticipated that the inclusion of this methyl group would not greatly affect the spectrum. Furthermore, it should be feasible to synthesize compound **17** without the methyl substituent; in this case, cation **16** should be generated directly in the dediazoniation reaction.

Concluding remarks

ab initio Molecular orbital theory has been used to design substituted phenyl cations that can be generated by dediazoniation and be directly observed by laser flash photolysis in solution. Heteroatom substitution external to the ring alters the orbital energies of the parent phenyl cation and results in several derived cations that are potentially observable but for various reasons, not ideal. Internal heterosubstitution introduces new transitions involving excitations of non-bonding electrons. In the most favourable cases, these transitions possess spectroscopic properties that are well suited for the specified purpose. A judicious combination of internal and external heteroatom substitution results in a synthetically accessible heterocyclic arenediazonium ion, which should lead to an aryl cation with a readily observable UV absorption spectrum. The ground is now cleared for experimental verification of the long-postulated involvement of aryl cations in dediazoniation reactions in solution, and an LFP investigation of the reactivity of aryl cations.

Acknowledgements

We thank the British Council and the Croatian Ministry of Science for a travel grant under the ALIS programme.

References

1 M. Speranza, *Tetrahedron Lett.*, 1980, **21**, 1983; G. Angelini, S. Fornarini and M. Speranza, *J. Am. Chem. Soc.*, 1982, **104**, 4773; M. Speranza, Y. Keheyan and G. Angelini, *J. Am. Chem. Soc.*, 1983, **105**, 6377; Y. Keheyan and M. Speranza, *Helv. Chim. Acta*, 1985, **68**, 2381; A. Filippi, G. Lilla, G. Occhiucci, C. Sparapani, O. Ursini and M. Speranza, *J. Org. Chem.*, 1995, **60**, 1250.
2 M. Winkler and W. Sander, *Angew. Chem., Int. Ed.*, 2000, **39**, 2014.
3 H. Zollinger, *Acc. Chem. Res.*, 1973, **6**, 335; H. Zollinger, *Diazo Chemistry I: Aromatic and Heteroaromatic Compounds*, VCH, New York, 1994; *The Chemistry of Diazonium and Diazo Groups*, ed. S. Patai, Interscience, New York, 1978; H. Maskill and K. McCrudden, *Croat. Chem. Acta*, 1992, **65**, 567; P. S. J. Canning, K. McCrudden, H. Maskill and B. Sexton, *Chem. Commun.*, 1998, 1971; P. S. J. Canning, K. McCrudden, H. Maskill and B. Sexton, *J. Chem. Soc., Perkin Trans. 2*, 1999, 2735; P. S. J. Canning, K. McCrudden, H. Maskill and B. Sexton, *Bull. Chem. Soc. Jpn.*, in press.
4 I. M. Cuccovia, M. A. da Silva, M. C. Ferraz, J. R. Pliego, J. M. Riveros and H. Chaimovich, *J. Chem. Soc., Perkin Trans. 2*, 2000, 1896.
5 J. C. Scaiano and N. Kim-Thuan, *Can. J. Chem.*, 1982, **60**, 2286; J. C. Scaiano and N. Kim-Thuan, *J. Photochem.*, 1983, **23**, 269.
6 S. Steenken, M. Ashokkumar, P. Maruthamuthu and R. A. McClelland, *J. Am. Chem. Soc.*, 1998, **120**, 11925.
7 S. Kobayashi, Y. Hori, T. Hasako, K. Koga and H. Yamataka, *J. Org. Chem.*, 1996, **16**, 5274; P. J. Stang and Z. Rappoport (eds.), *Dicoordinated Carbocations*, J. Wiley and Sons, Chichester, 1997.
8 R. W. Taft, *J. Am. Chem. Soc.*, 1961, **83**, 3350.
9 E. M. Evleth and P. M. Horowitz, *J. Am. Chem. Soc.*, 1971, **93**, 5636; H. H. Jaffé and G. F. Koser, *J. Org. Chem.*, 1975, **40**, 3082; J. D. Dill, P. v. R. Schleyer and J. A. Pople, *Tetrahedron Lett.*, 1975, 2857; J. D. Dill, P. v. R. Schleyer and J. A. Pople, *J. Am. Chem. Soc.*, 1977, **99**, 1; H. B. Ambroz and T. J. Kemp, *J. Chem. Soc., Perkin Trans. 2*, 1979, 1420.
10 A. Nicolaides, D. M. Smith, F. Jensen and L. Radom, *J. Am. Chem. Soc.*, 1997, **119**, 8083.
11 J. Hrusák, D. Schröder and S. Iwata, *J. Chem. Phys.*, 1997, **106**, 7541.
12 J. N. Harvey, M. Aschi, H. Schwarz and W. Koch, *Theor. Chem. Acc.*, 1998, **99**, 95; M. Aschi and J. N. Harvey, *J. Chem. Soc., Perkin Trans. 2*, 1999, 1059.
13 Gaussian 94, Revision E 2, M. J. Frisch, G. W. Trucks, H. B. Schlegel, P. M. W. Gill, B. G. Johnson, M. A. Robb, J. R. Cheeseman, T. Keith, G. A. Petersson, J. A. Montgomery, K. Raghavachari, M. A. Al-Laham, V. G. Zakrzewski, J. V. Ortiz, J. B. Foresman, J. Cioslowski, B. B. Stefanov, A. Nanayakkara, M. Challacombe, C. Y. Peng, P. Y. Ayala, W. Chen, M. W. Wong, J. L. Andres, E. S. Replogle, R. Gomperts, R. L. Martin, D. J. Fox, J. S. Binkley, D. J. Defrees, J. Baker, J. P. Stewart, M. Head-Gordon, C. Gonzalez and J. A. Pople, Gaussian, Inc., Pittsburgh, PA, 1995.
14 MOLPRO 2000 is a package of *ab initio* programs written by H.-J. Werner and P. J. Knowles with contributions from J. Almlof, R. D. Amos, A. Berning, D. L. Cooper, M. J. O. Deegan, A. J. Dobbyn, F. Eckert, S. T. Elbert, C. Hampel, R. Lindh, W. A. Lloyd, W. Meyer, A. Nickless, K. Peterson, R. Pitzer, A. J. Stone, P. R. Taylor, M. E. Mura, P. Pulay, M. Schütz, H. Stoll and T. Thorsteinsson.
15 MOLCAS Version 5, K. Andersson, M. Barysz, A. Bernhardsson, R. A. Blomberg, D. L. Cooper, T. Fleig, M. P. Fülscher, C. de Graaf, B. A. Hess, G. Karlström, R. Lindh, P.-Å. Malmqvist, P. Neogrády, J. Olsen, B. O. Roos, A. J. Sadlej, M. Schütz, B. Schimmelpfennig,

L. Seijo, L. Serrano-Andrés, P. E. M. Siegbahn, J. StÅlring, T. Thorsteinsson, V. Veryazov and P.-O. Widmark, Lund University, Sweden, 2000.
16 J. Finley, P.-Å. Malmqvist, B. O. Roos and L. Serrano-Andrés, *Chem. Phys. Lett.*, 1998, **288**, 299.
17 R. Glaser, *J. Phys. Chem.*, 1989, **93**, 7993; R. Glaser, G. S.-C. Choy and M. K. Hall, *J. Am. Chem. Soc.*, 1991, **113**, 1109; R. Glaser, *J. Comput. Chem.*, 1990, **11**, 663; R. Glaser and C. J. Horan, *J. Org. Chem.*, 1995, **60**, 7518.
18 R. Glaser, C. J. Horan, M. Lewis and H. Zollinger, *J. Org. Chem.*, 1999, **64**, 902.
19 R. N. Butler, *Chem. Rev.*, 1975, **75**, 241.
20 M. P. V. Boarland and J. F. W. McOmie, *J. Chem. Soc.*, 1951, 1218.
21 K. Yanai, *J. Pharm. Soc. Jpn.*, 1942, **62**, 315; K. Yanai, *Chem. Abstr.*, 1951, **45**, 5150i.
22 S. H. Chang, J. S. Kim and T. S. Huh, *Daerhan Hwahak Hwoejee*, 1969, **13**, 177; S. H. Chang, J. S. Kim and T. S. Huh, *Chem. Abstr.*, 1969, **71**, 112880j.